

A MODEL FOR THE CROSS SECTION OF A TURBULENT, RADIATIVE JET OR WAKE

J. Cantó,¹ A. C. Raga,² and A. Riera^{3,4}

Received 2003 February 10; accepted 2003 May 14

RESUMEN

Presentamos un modelo analítico de la sección de un flujo turbulento y radiativo. Este modelo es apropiado para modelar chorros HH o “estelas” detrás de “balas astrofísicas”. A pesar de que el modelo es muy simple, tiene la propiedad benigna de tener sólo cuatro parámetros libres (el radio exterior del flujo, la velocidad axial, la velocidad del borde del haz, y la dispersión de velocidades turbulentas), que pueden ser derivados mediante una comparación con las secciones de la velocidad radial y del ancho de línea de un objeto observado. Ilustramos como realizar este tipo de ajustes usando observaciones espectroscópicas previamente publicadas del chorro HH 110.

ABSTRACT

We present an analytical model for the cross section of a turbulent, radiative jet or wake. This model is appropriate for modeling HH jets, or “wakes” left behind by “astrophysical bullets”. Even though the model is very simple, it has the benign property of only having four free parameters (the outer radius of the beam, the axial velocity, the velocity at the edge of the beam, and the turbulent velocity width), which can be derived by fitting the radial velocity and line width cross sections of an observed outflow. We illustrate how to do such fits using previously published spectroscopic data of the HH 110 jet.

Key Words: **ISM: HERBIG-HARO OBJECTS — ISM: INDIVIDUAL (HH 110) — ISM: JETS AND OUTFLOWS — ISM: KINEMATICS AND DYNAMICS**

1. INTRODUCTION

Some HH jets show complex structures of emitting knots that are reminiscent of turbulent, laboratory jets. Two examples of this kind of flow are HH 111 (Reipurth, Raga, & Heathcote 1996) and HH 399 (Cernicharo et al. 1998; Rosado et al. 1999). The morphology of these jets resembles the radio continuum maps of Faranoff-Riley Type I extragalactic jets, which have been modeled in terms of analytical “mean flow+turbulent eddy” fully turbulent jet models (e.g., Bicknell 1984, 1986; Komissarov 1988, 1994).

For HH jets, some effort has been done to model the turbulent boundary layer around a laminar jet

beam core (e.g., Cantó & Raga 1991; Lim, Rawlings, & Williams 1999; Binette et al. 1999). However, models for a fully turbulent jet have been quite primitive (Richer, Hills, & Padman 1992; Raga et al. 1993), and limited to a description of the general dynamical properties of such a jet as it incorporates mass from the surrounding environment. Also, 2 and 3D numerical simulations of the development of turbulence in radiative jets have been carried out (Massaglia et al. 1996; Rossi et al. 1997; Downes & Ray 1998; Stone, Xu, & Hardee 1997; Xu, Hardee, & Stone 2000; Micono et al. 2000).

In the present paper, we discuss an analytical model for the cross section of a radiative, turbulent jet. Even though the model is dynamically very simple, it is useful in that it leads to concrete predictions of the observational properties (radial velocity, line widths and line profiles) that should characterize the cross section of a turbulent jet. The usefulness of this model is then illustrated by carrying out a compar-

¹Instituto de Astronomía, Universidad Nacional Autónoma de México, México.

²Instituto de Ciencias Nucleares, Universidad Nacional Autónoma de México, México.

³Departament de Física i Enginyeria Nuclear, Universitat Politècnica de Catalunya, Spain.

⁴On sabbatical leave at the ICN-UNAM.

ison with long-slit spectra of the HH 110 jet (taken from Riera et al. 2003a).

We present the dynamical model in § 2. The derivation of the line profiles and their moments (barycenter and line width) is discussed in § 3. The comparison with observations of HH 110 is made in § 4. Finally, the results are discussed in § 5.

2. A SIMPLE MODEL FOR A TURBULENT JET OR WAKE

It is common practice to describe a turbulent flow as a superposition of a “mean flow” (corresponding in principle to an ensemble average of many “experiments”, but which can also be estimated by appropriately defined spatial or temporal averages) and highly time-dependent and chaotic “turbulent eddies”. It is well known that both turbulent laboratory jets and turbulent wakes have an axially peaked mean flow velocity, which is directed mainly along the flow axis. Even though there are no experiments of radiative, high Mach number jets, 3D numerical simulations of such jets (e.g., Micono et al. 2000) appear to show that when such flows become turbulent, they also develop an axially peaked mean flow velocity profile.

In order to develop an analytical model of the cross section of the jet, we will then consider a Taylor series expansion $v_j(r) = a + br + cr^2 + \dots$ for the mean flow velocity (which we assume to be directed along the flow axis). It can be argued that in order not to have an unphysical axial “cusp”, the first order term has to be equal to zero. Therefore, the lowest order, physically meaningful, expansion is quadratic. We then consider the simplest possible form for the mean flow velocity cross section:

$$v_j(r) = v_0 \left(1 - \frac{r^2}{h^2} \right) + v_1, \quad (1)$$

where h is the outer radius of the jet beam, $v_0 + v_1$ is the axial velocity, and v_1 is the velocity of the material in the outer edge of the jet beam (with $r = h$). We will assume that h , v_0 , and v_1 vary only slowly along the beam of the jet (in other words, that they change over scales much larger than h), so that they can be considered as constants when studying the properties of the jet cross section.

Superimposed on this mean velocity, one also has the turbulent eddies. We will assume that these motions are randomly directed, and that the component of this velocity along any direction has a Gaussian probability distribution with a mean value of zero, and a dispersion Δv_T which is independent of position. For subsonic flows, it is normal to set

$\Delta v_T \propto v_j$. However, for supersonic flows it appears that laboratory experiments are consistent with a $\Delta v_T \propto c_s$ assumption (where c_s is the sound speed, —see Cantó & Raga 1991). As a radiative turbulent jet is approximately isothermal (see below), this leads to the conclusion that Δv_T should be independent of position.

As is normally done in models of turbulent jets, we will assume that the jet beam is in lateral pressure equilibrium with the surrounding material. Also, it has been previously argued (Cantó & Raga 1991; Raga et al. 1993) that a radiative, turbulent flow reaches a local balance between the turbulent dissipation and the radiative energy loss, and that because of the steepness of the cooling function this balance always leads to a temperature of a few thousand K. Therefore, the flow is approximately isothermal. Together with the pressure balance condition, this leads to the conclusion that the density of the jet has to be approximately constant across the beam of the jet.

If the temperature and density across the section of the jet are constant, it then appears to be reasonable to assume that the emission coefficient j associated with a given emission line is independent of position across the section of the jet. However, this is not necessarily true for the emission lines which are responsible for the radiative cooling (e.g., the [O I], [O II], [C II] collisionally excited lines), which actually force the near isothermality through their strong temperature dependence. The assumption of a position-independent j is therefore only reasonable for lines such as the recombination lines of H, which have a temperature dependence which is much shallower than the one of the forbidden lines which dominate the radiative cooling of the gas. In the following, we also assume that the emission line under consideration (which could be, e.g., H α) is optically thin.

In this way, one can construct what is basically the simplest possible model for the mean flow cross section of a radiative turbulent jet or of a wake (which are completely equivalent at the level of approximation of the present model). This flow has a quadratic velocity profile (see eq. 1), and a position-independent line emission coefficient and turbulent velocity dispersion Δv_T . From this simple structure, one can then compute the emitted line profiles. This is done in the following section.

3. THE EMISSION LINE PROFILES

Let us consider an observation of a jet which is moving at an angle ϕ with respect to the plane of

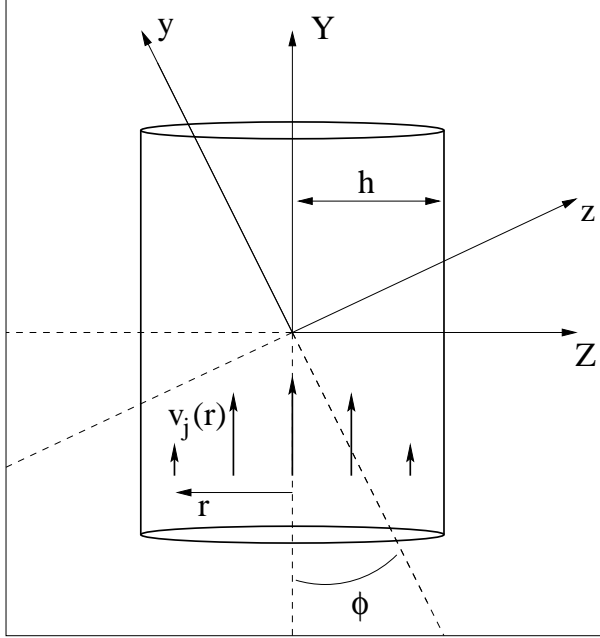


Fig. 1. Schematic diagram showing a turbulent jet with a mean flow velocity v_j that decreases monotonically as a function of the cylindrical radius r . The jet travels along the Y -axis. The X -axis, which is parallel to the plane of the sky, points out of the page, directly towards the reader. A second coordinate system is defined, with the z -axis along the line of sight, and the y -axis on the projection on the plane of the sky of the jet axis. The jet is shown moving at a (negative) angle ϕ (with respect to the plane of the sky) towards the observer.

the sky (with negative values of ϕ corresponding to motions towards the observer). One can construct an orthogonal coordinate system (X, Y, Z) , with the jet moving along the Y -axis and with the X -axis on the plane of the sky. The observer defines a second, (x, y, z) coordinate system, with y along the projection on the plane of the sky of the jet axis, x across the projected cross section of the jet, and z along the line of sight. These two coordinate systems are shown in the schematic diagram of Figure 1.

The component along z of the mean flow velocity (i.e., the radial velocity associated with the mean flow) then is:

$$v_m(x, z) = v_0 \sin \phi \left(1 - \frac{x^2 + z^2 \cos^2 \phi}{h^2} \right) + v_1 \sin \phi, \quad (2)$$

as can be deduced from eq. (1) and simple geometric relations between the (X, Y, Z) and (x, y, z) coordinates.

The radial velocity-dependent emission line coef-

ficient is then given by

$$j_v(x, z) = j_0 \Psi_v(x, z), \quad (3)$$

where j_0 is constant (see § 2) and

$$\Psi_v = \frac{1}{\sqrt{\pi} \Delta v} e^{-(v-v_m)^2/\Delta v^2}, \quad (4)$$

where v_m is given by eq. (2) and the velocity dispersion Δv includes both the turbulent and the thermal motions of the gas. Also, in order to compare predictions of the model with observations, one can include the instrumental broadening by adding it in quadrature to the thermal+turbulent line width.

The specific intensity along a line of sight passing at a distance x from the projected outflow axis is then given by

$$I_v(x) = 2 \int_0^{z_m} j_0 \Psi_v dz, \quad (5)$$

where

$$z_m = \frac{(h^2 - x^2)^{1/2}}{\cos \phi}. \quad (6)$$

For non-zero Δv , the integral of eq. (5) cannot be performed analytically. In order to calculate it numerically, we can write it in dimensionless form:

$$I_\nu = \frac{1}{\Delta \nu} \int_0^1 e^{-[\nu - (1-\eta^2)]^2/\Delta \nu^2} d\eta, \quad (7)$$

where $\eta = z/z_m$ and

$$I_\nu = \frac{\sqrt{\pi} v_0 \sin \phi \cos^2 \phi z_m^2}{2 j_0 h^2} I_\nu, \quad (8)$$

$$\nu = \frac{h^2 (v - v_1 \sin \phi)}{v_0 \sin \phi \cos^2 \phi z_m^2}, \quad (9)$$

$$\Delta \nu = \frac{h^2 \Delta v}{v_0 \sin \phi \cos^2 \phi z_m^2}. \quad (10)$$

In the $\Delta \nu \rightarrow 0$ limit, the integral of eq. (7) can be performed analytically, giving

$$I_\nu \rightarrow \frac{\sqrt{\pi}}{2\sqrt{1-\nu}}. \quad (11)$$

For nonzero $\Delta \nu$ one can compute the dimensionless line profiles by carrying out a numerical integration of eq. (7). Alternatively, one could compute the same line profile by convolving eq. (11) with a Gaussian of dispersion $\Delta \nu$ (which one can prove is mathematically equivalent to eq. 7). The results of such integrations are shown in Figure 2.

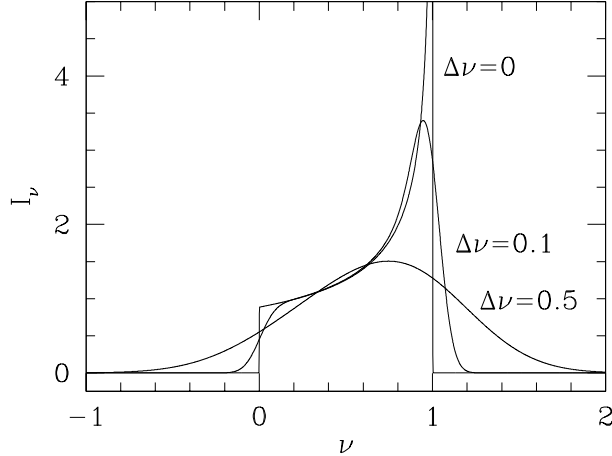


Fig. 2. Dimensionless line profiles I_ν (see eq. 7) as a function of the dimensionless radial velocity ν (see eq. 9) for three different values of the dimensionless turbulent+thermal line width $\Delta\nu$ (see eq. 10). The solution for $\Delta\nu = 0$ is given analytically by eq. (11).

We now compute three different velocity-moments of the line profile (given by eq. 5). The line flux is:

$$I_0 \equiv \int_{-\infty}^{\infty} I_\nu(x) d\nu = 2j_0 z_m = 2j_0 \frac{(h^2 - x^2)^{1/2}}{\cos \phi}. \quad (12)$$

The barycenter of the line profile is given by:

$$\begin{aligned} V_c &\equiv \frac{1}{I_0} \int_{-\infty}^{\infty} \nu I_\nu(x) d\nu \\ &= \frac{2}{3} v_0 \sin \phi \frac{(h^2 - x^2)}{h^2} + v_1 \sin \phi. \end{aligned} \quad (13)$$

Finally, the velocity dispersion of the line profile is:

$$\begin{aligned} W^2 &\equiv \frac{1}{I_0} \int_{-\infty}^{\infty} (\nu - V_c)^2 I_\nu(x) d\nu \\ &= \frac{\Delta\nu^2}{2} + \frac{4}{45} v_0^2 \sin^2 \phi \left(1 - \frac{x^2}{h^2}\right)^2. \end{aligned} \quad (14)$$

These expressions for the line center (eq. 13) and for the line width (eq. 14), as well as the shape of the line profile itself (eq. 5), can in principle be compared directly with observations of turbulent, radiative astrophysical jets. In the following section, we show such a comparison between our model and previously published observations of HH 110.

4. A COMPARISON WITH OBSERVATIONS OF HH 110

Riera et al. (2003a) obtained high resolution, long-slit spectra across knots B and C of the HH 110

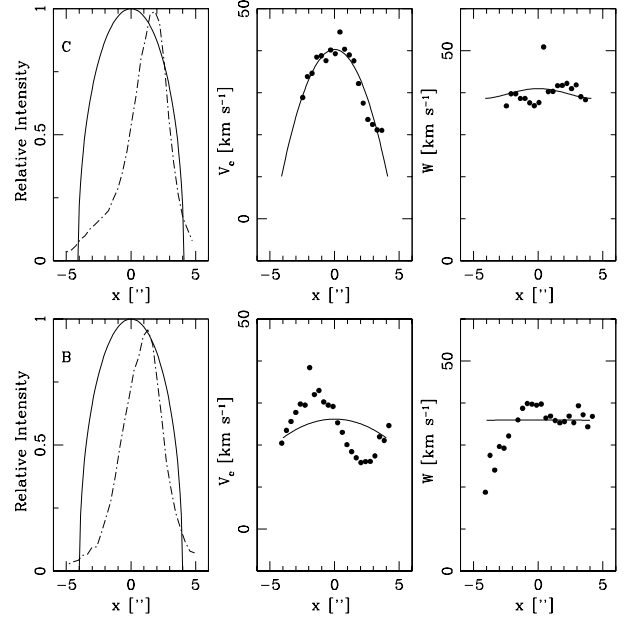


Fig. 3. $H\alpha$ intensity (dashed line, left), barycenters (dots, centre) and line widths (dots, right) as a function of position across the width of the HH 110 jet, obtained from the long-slit spectra of Riera et al. (2003a). The results obtained for slit positions across knot B (bottom) and knot C (top) are shown. The abscissa gives the position as offsets from the outflow axis. The observed radial velocities are given relative to the velocity of the nearby molecular cloud, and are plotted as positive values (the HH 110 flow, however, is blue-shifted). The solid lines show the results from the model fits described in § 3 (see also Table 1).

jet (which lie at distances of ≈ 8 and $23''$ down the jet axis from knot A). From the resulting $H\alpha$ position-velocity (PV) diagrams, we can compute the barycenter and width of the line profiles (using the first equalities of eqs. 13 and 14, respectively) as a function of position across the jet axis.

The obtained results are shown in Figure 3. From this figure, we see that for knot C one obtains a centrally peaked $V_c(x)$ cross section, and a flat $W(x)$ dependence. For knot B, one obtains a more complex, asymmetric $V_c(x)$ cross section.

We now proceed as follows. We fix the width of the jet to a value $h = 4''$ (which approximately corresponds to the half-width of the region with observed emission). Then, we carry out a least squares fit of the $V_c(x)$ dependence predicted from the model (eq. 13) in order to obtain the values of $v_0 \sin \phi$ and $v_1 \sin \phi$ which best fit the data. Finally, using these values for h , $v_0 \sin \phi$ and $v_1 \sin \phi$, we carry out a fit to the observed line widths with the $W(x)$ predicted from the model (eq. 14) in order to determine the

TABLE 1
MODEL FITS TO HH 110^a

Knot	h ["]	$v_0 \sin \phi$	$v_1 \sin \phi$	$v_0 + v_1$ ^b [km s ⁻¹]	Δv
B	4	7	22	50	51
C	4	45	10	97	55

^aFits to the long-slit spectra across knots B and C obtained by Riera et al. (2003a).

^bComputed for an orientation angle $\phi = -35^\circ$ with respect to the plane of the sky.

value of Δv . In this way, we determine the parameters of the model that best fit the observed cross sections of the HH 110 jet.

The model parameters resulting from these fits are given in Table 1. For knot B, the least squares fit gives a flat $V_c(x)$ cross section, which does not reproduce well the rather complex, observed cross section (see Figure 3). On the other hand, a more convincing fit is obtained for the $V_c(x)$ cross section of knot C. For both knots B and C, the observed H α intensity cross sections are much sharper and more asymmetric than the broader, symmetric intensity cross section predicted from the model.

The model fits show an outward “acceleration”, with a higher axial velocity for knot C than for knot B. This result is in agreement with the acceleration down the jet axis noted by Riera et al. (2003a). On the other hand, the model fits to both knots give similar, $\Delta v \sim 50$ km s⁻¹ line broadenings (see eq. 4 and Table 1). This line broadening clearly exceeds the 20 km s⁻¹ instrumental broadening of the data of Riera et al. (2003a), and therefore mostly reflects the turbulent motions of the gas flowing down the HH 110 flow.

Using these model fits, we can now calculate predicted PV diagrams (for a slit position across the jet axis) by numerically integrating eq. (5). We then convolve the model predictions with a Gaussian “seeing” of FWHM = 2".5 in order to simulate the conditions of the observations of Riera et al. (2003a). The results of this exercise are shown in Figure 4, together with the observed H α PV diagrams for knots B and C.

Comparing the predicted and observed PV diagrams, one sees that while their general characteristics (e.g., the radial velocities, characteristic line widths and spatial extension of the emission) agree well (as guaranteed by the model fits described above), they do have substantial differences. In particular, the observed PV diagrams show clear asym-

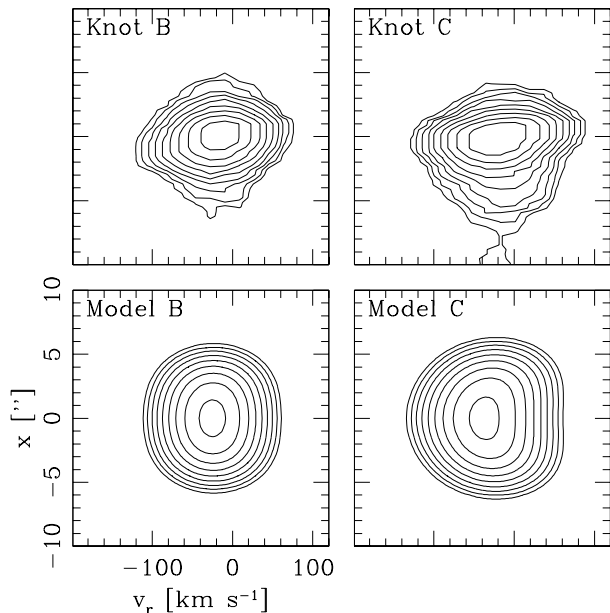


Fig. 4. Observed (top) and predicted (bottom) H α PV diagrams for knots B (left) and C (right). The radial velocities of the observed PV diagrams are given with respect to the radial velocity of the nearby molecular cloud. The positions are given as offsets across the jet beam, measured from the outflow axis. The PV diagrams are depicted with logarithmic, $\sqrt{2}$ contours.

metries on the two sides of the outflow axis, which are of course absent in the axisymmetric theoretical model.

5. CONCLUSIONS

We have developed a simple, analytical model that describes the cross section of a radiative, turbulent flow. This flow could correspond to a turbulent jet beam, or to a turbulent wake left behind by the passage of an “astrophysical bullet”.

Though the model is extremely simple, it has the redeeming property that it leads to clear, analytic predictions of the spatial dependence (across the outflow) of the emission line profiles. In particular, we derive relations giving the barycenter and the line width as a function of position across the outflow.

We have then shown how these relations can be used to model the observed cross sections of the HH 110 jet (taken at two different positions along the jet beam). From fits to the observed barycenter and line widths, one can derive the four free parameters of the model: the outer radius of the beam, the central velocity, the velocity of the outer edge of the beam and the “turbulent width” of the emitted lines.

Interestingly, we find that while the observed ra-

dial velocity cross section of knot C (of HH 110) does resemble the functional form predicted by our model, the cross section of knot B does not (see Fig. 3). This kind of result is not surprising, since a truly turbulent flow will have eddies of all sizes (up to sizes comparable to the width of the jet). Therefore, comparisons of observed cross sections (taken at a given position along the jet) with predictions from a “mean flow model” (in which the turbulent eddies are only considered in the form of a line broadening) are likely to be unsatisfactory.

In order to obtain more appropriate comparisons between our analytical model and observations of HH jets it would be necessary to have spectroscopic observations with 2D spatial resolution. With such observations, one could calculate jet cross sections from the emission averaged over an appropriately defined length along the outflow axis. This “averaging length” should be larger than a few jet diameters, so that an average over several characteristic sizes of the turbulent eddies is carried out.

In this way, one could try to recover the properties of the “mean flow” from observations of a turbulent jet or wake. With such results, a more appropriate comparison with the model described above could be carried out.

This has now been attempted by Riera et al. (2003b), who have obtained Fabry-Pérot observations of HH 110, and computed cross sections of the outflow carrying out averages along the jet over the sizes of the different emission structures (using a wavelet analysis technique). These authors find that such “average cross sections” compare surprisingly well with the cross sections predicted by the analytic model described above. This somewhat surprising result appears to indicate that our simple model does capture some of the important properties of the HH 110 flow.

The work of JC and ACR was supported by CONACyT grants 36572-E and 34566-E. A. Riera acknowledges the ICN-UNAM for support during her

sabbatical. The work of A. Riera was supported by the MCyT grant AYA2002-00205 (Spain). We acknowledge an anonymous referee for helpful comments.

REFERENCES

- Bicknel, G. V. 1984, *ApJ*, 286, 68
 _____ 1986, *ApJ*, 305, 109
 Binette, L., Cabrit, S., Raga, A. C., & Cantó, J. 1999, *A&A*, 346, 260
 Cantó, J., & Raga, A. C. 1991, *ApJ*, 372, 646
 Cernicharo, J., Lefloch, B., Cox, P., Cesarsky, D., Esteban, C., Yusef-Zadeh, F., Méndez, D. I., Acosta-Pulido, J., & García López, R. J. 1998, *Sci.*, 282, 462
 Downes, T. P., & Ray, T. P. 1988, *A&A*, 331, 1130
 Komissarov, S. S. 1988, *Ap*, 28, 154
 _____ 1994, *MNRAS*, 269, 394
 Lim, A. J., Rawlings, J. M. C., & Williams, D. A. 1999, *MNRAS*, 308, 1126
 Massaglia, S., Rossi, P., Bodo, G., & Ferrari, A. 1996, *ApL&C*, 34, 295
 Miccono, M., Massaglia, S., Rossi, P., Ferrari, A., & Rosner, R. 2000, *A&A*, 360, 795
 Raga, A. C., Cantó, J., Calvet, N., Rodríguez, L. F., & Torrelles, J. M. 1993, *A&A*, 276, 539
 Reipurth, B., Raga, A. C., & Heathcote, S. 1996, *A&A*, 311, 989
 Richer, J. S., Hills, R. E., & Padman, R. 1992, *MNRAS*, 254, 525
 Riera, A., López, R., Raga, A. C., Estalella, R., & Anglada, G. 2003a, *A&A*, 400, 213
 Riera, A., Raga, A. C., Reipurth, B., Amram, Ph., Boulesteix, J., Cantó, J., & Toledano, O. 2003b, *AJ*, in press
 Rosado, M., Esteban, C., Lefloch, B., Cernicharo, J., & García López, R. J. 1999, *AJ*, 118, 2962
 Rossi, P., Bodo, G., Massaglia, S., & Ferrari, A. 1997, *A&A*, 321, 672
 Stone, J. M., Xu, J., & Hardee, P. E. 1997, *ApJ*, 483, 136
 Xu, J., Hardee, P. E., & Stone, J. M. 2000, *ApJ*, 543, 161

Jorge Cantó: Instituto de Astronomía, UNAM, Apdo. Postal 70-264, 04510 México, D. F., México.

Alejandro C. Raga: Instituto de Ciencias Nucleares, UNAM, Apdo. Postal 70-543, 04510 México, D. F., México. (raga@nuclecu.unam.mx).

Angels Riera: Departament de Física i Enginyeria Nuclear, Universitat Politècnica de Catalunya, Av. Víctor Balaguer s/n, E-08800 Vilanova i la Geltrú, Spain. (angels.riera@upc.es).